CASE REPORT

AMERICAN JOURNAL OF
medical genetics A | WILEY

A de novo *ACTB* gene pathogenic variant in identical twins with phenotypic variation for hydrops and jejunal atresia

Kristina Sibbin[1] | Patrick Yap[1] | Denis Nyaga[2] | Raoul Heller[1] | Stephen Evans[1] | Kate Strachan[1] | Salam Alburaiky[1] | Han M. (Alex) Nguyen[3] | Sylvie Hermann-Le Denmat[3] | Austen R. D. Ganley[3] | Justin M. O'Sullivan[2,4,5,6,7] | Frank H. Bloomfield[1,2]

[1]Starship Child Health, Auckland City Hospital, Auckland, New Zealand

[2]Liggins Institute, The University of Auckland, Auckland, New Zealand

[3]School of Biological Sciences, The University of Auckland, Auckland, New Zealand

[4]The Maurice Wilkins Centre, The University of Auckland, Auckland, New Zealand

[5]Australian Parkinsons Mission, Garvan Institute of Medical Research, Sydney, New South Wales, Australia

[6]Brain Research New Zealand, The University of Auckland, Auckland, New Zealand

[7]MRC Lifecourse Epidemiology Unit, University of Southampton, Southampton, UK

Correspondence
Frank H. Bloomfield, Liggins Institute, University of Auckland, Private Bag 92019, Auckland 1142, New Zealand.
Email: f.bloomfield@auckland.ac.nz

Abstract

The beta-actin gene (*ACTB*) encodes a ubiquitous cytoskeletal protein, essential for embryonic development in humans. De novo heterozygous missense variants in the *ACTB* are implicated in causing Baraitser–Winter cerebrofrontofacial syndrome (BWCFFS; MIM#243310). *ACTB* pathogenic variants are rarely associated with intestinal malformations. We report on a rare case of monozygotic twins presenting with proximal small bowel atresia and hydrops in one, and apple-peel bowel atresia and laryngeal dysgenesis in the other. The twin with hydrops could not be resuscitated. Intensive and surgical care was provided to the surviving twin. Rapid trio genome sequencing identified a de novo missense variant in *ACTB* (NM_00101.3:c.1043C>T; p.(Ser348Leu)) that guided the care plan. The identical variant subsequently was identified in the demised twin. To characterize the functional effect, the variant was recreated as a pseudoheterozygote in a haploid wild-type *S. cerevisiae* strain. There was an obvious growth defect of the y*ACT1*$^{S348L/WT}$ pseudoheterozygote compared to a y*ACT1*$^{WT/WT}$ strain when grown at 22°C but not when grown at 30°C, consistent with the y*ACT1* S348L variant having a functional defect that is dominant over the wild-type allele. The functional results provide supporting evidence that the Ser348Leu variant is likely to be a pathogenic variant, including being associated with intestinal malformations in BWCFFS, and can demonstrate variable expressivity within monozygotic twins.

KEYWORDS
ACTB, actin, apple-peel bowel, Baraitser–Winter, jejunal atresia

1 | INTRODUCTION

Baraitser–Winter cerebrofrontofacial syndrome (BWCFFS) is a rare, and likely underdiagnosed, condition first described in 1988 (Baraitser & Winter, 1988) with fewer than 100 cases reported worldwide. BWCFFS is characterized by recognizable craniofacial dysmorphism with hypertelorism, ptosis, metopic ridging and ocular colobomata, intellectual disability, and congenital brain malformations. There is significant variable expressivity in other associated phenotypic characteristics, including growth delay and/or short stature,

various congenital cardiac and genitourinary malformations, and pectus deformities, which can make prompt perinatal diagnosis challenging. Rapid trio whole genome sequencing (WGS) is emerging as a high-yield diagnostic clinical tool that provides early accurate diagnosis in critically ill infants, informing planning of medical management. The utility of WGS may extend to include infants with BWCFFS at the severe end of the phenotypic spectrum.

Pathogenic variants in the actin-encoding *ACTB* and *ACTG1* have been identified that are suggested to underlie the syndrome (Riviere et al., 2012; Verloes et al., 2015; Yates et al., 2017). Beta-actin is a highly conserved cytoskeletal protein that is ubiquitously expressed and essential for cell migration, mitosis, intracellular transport, and cell maintenance (Dominguez & Holmes, 2011). The likely pathogenic role of actin variants is highlighted by the finding that a variant in the *ACTB* gene leads to mutant actin within cells and has a molecularly proven actinopathy (Johnston et al., 2013). The severity and distribution of mutant actin within cells, and where the variant is located within the protein, may dictate the extent of abnormal development and the phenotypic variability among patients (Sandestig et al., 2019).

Several patients with an *ACTB* variant, including c.1043C>T; p. (Ser348Leu), have been reported to have associated malformations of the small bowel, including a patient with apple-peel jejunal atresia (Fakhro et al., 2019; Saskin et al., 2017). Jejunoileal atresia with an "apple-peel" small bowel deformity is a rare form of intestinal atresia that comprises distal duodenal or proximal jejunal atresia and an associated arteriopathy, with a spiraling appearance of the small bowel distal to the obstruction. Various potential etiologies have been proposed, including vascular insults, a failure of recanalization of the bowel lumen and, given an increased incidence in some families (Kirtane et al., 2019) and associated congenital malformations (Dalla Vecchia et al., 1998), a monogenic etiology.

We report on monozygotic twins with differing clinical phenotypes in whom an *ACTB* missense variant was identified through proband-parents rapid trio whole WGS. We performed a functional assay to characterize the effect of the *ACTB* variant in yeast, providing evidence to support its disease-causing role, confirmed as BWCFFS.

2 | MOLECULAR METHODS

2.1 | Whole genome sequencing

Rapid proband-parents trio WGS and data analysis were performed by Victorian Clinical Genetics Service Clinical Genomics Laboratory, Victoria, Australia following pretest counseling and informed consent obtained by the Genetics Health Service New Zealand. Autonomy of the probands as infants was safe-guarded throughout. Whole genome sequencing was performed using massively parallel sequencing (NexteraTM DNA Flex Library Prep kit, Illumina Sequencers) with a mean target coverage of $30\times$ and a minimum of 90% of bases sequenced to at least $10\times$. Data were processed, including read alignment to the reference genome (GRCh38) and variant calling, using Cpipe (Sadedin et al., 2015), or via functionally equivalent analysis

with the Illumina Dragen System. Variant analysis and interpretation within the selected target region (RefSeq genes ±1Kb) was performed using Agilent Alissa Interpret. Variants were annotated against all RefSeq gene transcripts and reported in accordance with Human Genome Variation Society nomenclature. Copy number variants (CNV) were screened for using an internal CNV detection tool, CxGo (Sadedin et al., 2018).

2.2 | Synthesis of the yeast $ACT1^{S348L}$ allele

The *S. cerevisiae* *ACT1* gene (formerly called YFL039C; hereafter y*ACT1*) was synthesized with two nucleotide substitutions (CT>TG at positions 1043/4) that change the codon 348 amino acid from serine to leucine (S348L) to produce the same amino acid substitution as in humans (Table S1, Supporting Information). The resulting $ACT1^{S348L}$ allele was cloned as a *Xba*I/BamHI fragment in the pUC57 vector, giving plasmid p(S348L) (GenScript, Singapore). p(S348L) was amplified in *Escherichia coli* DH5α cells (Mix and Go *E. coli* Transformation Kit; Zymo Research, Irvine, CA). Plasmid DNA was extracted from single colonies using the NucleoSpin plasmid kit (MediRay, Auckland, NZ). Five microgram of p(S348L) DNA was digested (37°C, 3 h) with 10 U *Bam*HI and 10 U *Eco*RI (NEB, Ipswich, MA), and the 2 kb *Bam*HI/*Eco*RI DNA fragment band corresponding to y$ACT1^{S348L}$ was gel extracted and purified (Gel and PCR clean-up kit, Macherey-Nagel, Dueren, Germany).

2.3 | DNA amplification of the $yACT1^{WT}$ wild-type allele

$yACT1^{WT}$ was PCR amplified from genomic DNA extracted from *S. cerevisiae* strain NOY408-1b (*MATa ade2-1 ura3-1 his3-11 trp1-1 leu2-3112 can1-100*) (Ganley et al., 2009) using primers Act1_Full-F and Act1_Full-R (Table S2) (98°C, 2 min, 30× [98°C, 30 s; 54°C, 30 s; 72°C, 2 min]) and the high fidelity Q5 DNA polymerase (NEB). Five microgram of the PCR amplified DNA was digested (37°C, 3 h) with 10 U *Bam*HI and 10 U *Pst*I, and purified (Gel and PCR clean-up kit, Macherey-Nagel).

2.4 | Cloning of $yACT1^{WT}$ and $yACT1^{S348L}$ into yeast centromeric plasmid

The *Bam*HI/*Pst*I $yACT1^{WT}$ DNA fragment was cloned into the yeast centromeric plasmid YCplac33 (*CEN4*, *URA3*) that was linearized by double restriction digestion (5 μg YCplac33, 10 U *Bam*HI, 10 U *Pst*I 37°C, 1 h). The *Bam*HI/*Eco*RI $yACT1^{S348L}$ DNA fragment was cloned into the yeast centromeric plasmid YCplac33 (*CEN4*, *URA3*) that was linearized by double restriction digestion (5 μg YCplac33, 10 U *Bam*HI, 10 U *Eco*RI 37°C, 1 h), and dephosphorylated (1 U rAPid Alkaline Phosphatase [Sigma], 37°C, 10 min). Ligations were performed mixing vector: insert at a ∼1:7 ratio (1UT4 DNA ligase, 16°C, overnight)

(Figure S1). Ligations mixtures were transformed into *E. coli* DH5α and positive clones were identified using colony PCR (95°C, 5 min, 30× [95°C, 30 s; 55°C, 15 s; 68°C, 60 s]) with M13-F and M13-R primers (Table S2) and KAPA2G Robust PCR kit (Roche). Plasmid DNA was extracted (NucleoSpin Plasmid kit) and the sequence of *yACT1*^{WT} and *yACT1*^{S348L} confirmed by Sanger sequencing (Auckland Genomics Centre, The University of Auckland, New Zealand) using primers M13-F, M13-R, ACT1_int-F and ACT1_int-R (Table S2).

2.5 | Transformation of pYCplac33:*yACT1*^{S348L} and pYCplac33:*yACT1*^{WT} into *S. cerevisiae*

Transformation of *S. cerevisiae* strain NOY408-1b was performed using the PEG-lithium acetate method (Kawai et al., 2010). Prior to transformation, 20 μg of denatured carrier DNA (salmon testis DNA) was mixed with 5 μg of plasmid DNA and added to competent NOY408-1B cells. All transformations, including controls, were plated onto glucose minimum medium supplemented with the appropriate nutritional requirements excepted uracil (SD-URA medium). SD-URA elective plates were incubated at 30°C for 3 days.

2.6 | Assessment of *yACT1*$^{S348L/WT}$ impact on *S. cerevisiae* cell growth

Two independent *S. cerevisiae* NOY408-1B YCplac33:*yACT1*^{S348L} colonies and two independent YCplac33:*yACT1*^{WT} colonies were grown in SD-URA medium at 30°C. To measure growth on plates, culture density was standardized to $OD_{600nm} = 0.6$ by dilution with SD-URA medium, and 5 μL of a 10-fold dilution series were spotted onto SD-URA plates. These were incubated at 30°C or room temperature (∼22°C) for 2 and 4 days, respectively. To measure growth in liquid culture, culture density was standardized to $OD_{600nm} = 0.4$, diluted ×100 with SD-URA, and 10 technical replicates of 200 μL of each sample were transferred to Bioscreen C growth analyser plates (Bioscreen C MBR, Oy Growth Curves Ab Ltd.). These were incubated at 30 or 22°C, and OD_{600nm} was monitored every 15 min for 48 h.

3 | EDITORIAL POLICIES AND ETHICAL CONSIDERATIONS

Written consent was obtained for publication of patient medical information and unmasked photographs.

4 | CLINICAL REPORT

The patients were naturally conceived monochorionic-diamniotic twins born to nonconsanguineous parents (mother 31 years old; father 35 years old) of Polynesian descent. There was no significant obstetric or family history. Maternal booking body mass index was 48 kg/m^2; a glucose tolerance test was normal. Small bowel atresia was suspected in both twins at 22 weeks' gestation when dilated stomach and proximal small bowel ("double-bubble") were noted on ultrasonography. Craniofacial features, including brachycephaly and flattened facial profile, and femur lengths on the 10th and 5th percentile in Twin 1 and Twin 2, respectively, also were identified on ultrasonogram. Amniocentesis was declined. Twin 1 developed fetal hydrops with bilateral pleural effusion and ascites at 26 weeks' gestation which by 29.5 weeks was severe with large pleural effusions, ascites, and skin edema. Abnormal Dopplers, with an absent "a" wave in the ductus venosus and absent end diastolic flow in the umbilical artery of Twin 1, suggested fetal demise of Twin 1 was imminent. Antenatal corticosteroid and magnesium sulfate were administered and the twins were delivered by emergency Caesarean section at 29.5 weeks.

Twin 1 was born in poor condition with no spontaneous movement and an Apgar score of 1 (heart rate <100/min). She had severe generalized subcutaneous edema with a birth weight 2375 g (>99th centile), length 41 cm (88th centile) and head circumference 30.5 cm (>99th centile). There was no response to extensive resuscitation and the baby died at 1 h of age. On post mortem examination, craniofacial features, including flat and broad nasal bridge, anteverted nasal tip, and tented upper lip (Figure 1a) were noted. Small bowel atresia was confirmed at the proximal jejunum, and the remaining small bowel was dilated. The mesentery appeared normal with no evidence of apple-peel bowel anomaly or additional segments of atresia (Figure 1d,e). The patient had severe pulmonary hypoplasia with a combined lung weight of 6.3 g (50th percentile for 29 weeks ∼20 g; Figure 1c). There was a single coronary ostium. The brain was not examined for malformations.

Twin 2 was born with a birth weight of 1210 g (40th centile), length 38 cm (49th centile), and head circumference 27.8 cm (78th centile). Observed craniofacial features included down-slanting palpebral fissures and a broad nasal bridge (Figure 1g). On Day 1, she was intubated for respiratory distress with exceptional difficulty. A small malformed larynx was seen. On Day 7, she was extubated to continuous positive airway pressure, which she did not tolerate. Otorhinolaryngology (ORL) review revealed laryngeal dysgenesis, primitive vocal folds and a malformed narrow proximal trachea, resulting in a critical airway necessitating a tracheostomy for ongoing care with need for later reconstructive surgery, meaning early decannulation would not be possible.

Early abdominal radiographs demonstrated a dilated stomach and proximal small bowel. On Day 2, laparotomy identified proximal jejunal atresia with an apple-peel bowel anomaly (Figure 1h,i). There was loss of the superior mesenteric artery (SMA) beyond the right colic branch and a large mesenteric defect, consistent with type IIIb jejunal atresia. The apple-peel segment was precariously supplied by a proximal marginal vessel. No additional small bowel atresia was identified. The colonic fixation was abnormal with the ileocecal junction passing behind the root of the mesentery and a malrotated, mechanically obstructed cecum in the left upper quadrant. Attempted correction of the malrotation resulted in obstruction of the SMA and poor perfusion to the apple-peel segment. Resection of the long jejunal atresia with
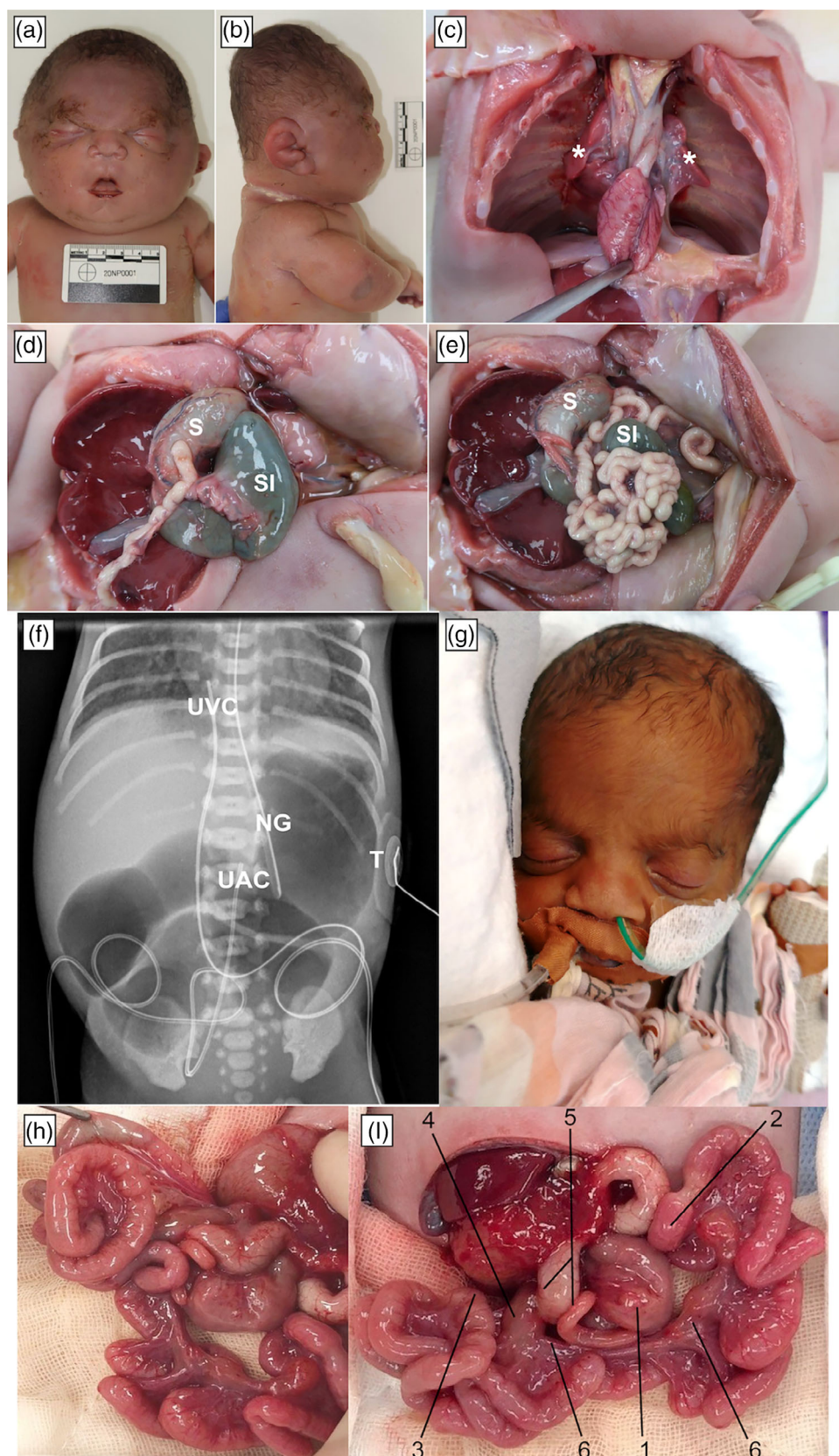
FIGURE 1 Clinical images of the twins, Twin 1 (a–e), Twin 2 (f–i). Severe hydrops is shown in (a, b), brachcephaly seen in (b). Profoundly small lungs in (c) marked by the asterisk (heart reflected). Dilated stomach and proximal small intestine are seen in (d, e). Radiograph on Day 1 in Twin 2 (f): dilated stomach and proximal small intestine. (g) Frontal facial view of intubated Twin 2; (h, i) intraoperative photographs. 1, proximal atretic jejunum; 2, distal end of jejunal atresia; 3, distal small intestine; 4, root of mesentery; 5, cecum and appendix; 6, marginal artery adjacent to the mesenteric defect supplying the "apple-peel" bowel. NG, nasogastric tube; S, stomach; SI, small intestine; UAC, umbilical arterial catheter; UVC, umbilical venous catheter; T, temperature sensor

side-to-side jejunojejunal anastomosis, devolving of the apple-peel bowel through 360 degrees and an ileostomy with a mucous fistula was therefore performed. Additional abnormalities included megakaryocytes, persistent hyperglycemia with a normal C-peptide concentration and normal head of pancreas on ultrasound, a large patent ductus arteriosus, and a small muscular ventricular septal defect.

In view of the precarious blood supply to the apple-peel segment, critical airway requiring a tracheostomy, presence of other unexplained phenotypic and clinical features and the demise of the co-twin from congenital anomalies, rapid proband-parents trio WGS and phenotype-driven, gene-prioritized data analysis were performed on Twin 2 with an anticipated turn-around time of 72 h. Earlier cytogenic analysis in both twins had reported unremarkable 46, XX karotypes and, in Twin 2, an SNP-array (Affymetric Cytoscan 750k) did not detect any significant imbalances. A de novo missense variant in *ACTB* was identified (NM_001101.3:c.1043C>T;p.(Ser348Leu)), classified as "likely pathogenic" (class 4). Ser348 lies in the C-terminal domain adjacent to the target binding domain (Dominguez & Holmes, 2011), where it appears to be intolerant of missense changes (missense constraint Z-score is 5.02). Furthermore, the Ser348Leu variant is absent from gnomAD and the majority of computational software predicts the variant as deleterious or damaging. The identical variant was subsequently identified in Twin 1 following analysis of stored genome data performed with parental consent. No other class 4 or 5 variants were identified.

On Day 13, Twin 2 developed Staphylococcal sepsis with septic thrombus obstructing the superior vena cava from a percutaneous central venous catheter inserted on Day 3 after birth. Given the predicted poor outcome and the additional impact of the diagnosis of BWCCFS on her health and development, the parents made an informed decision that palliative care was the appropriate option. She died on Day 23. Postmortem whole body MRI, with particular attention to the brain, did not detect any additional malformations.

5 | FUNCTIONAL STUDIES

The patients described in this study are heterozygous and therefore the mutation is likely dominant. To provide evidence supporting this variant in causing a developmental defect, we designed a pseudoheterozygote *S. cerevisiae* strain. This involved cloning the *S. cerevisiae* ortholog of *ACTB*, *yACT1*, with and without a S348L variant, into a yeast centromeric plasmid. The plasmid was then incorporated into a haploid *S. cerevisiae* strain. The centromeric plasmid was maintained as single copy. The *yACT1* is effectively diploid, whereas the remainder of the genome is haploid, hence creating a pseudoheterozygote *S. cerevisiae* strain. There was an obvious growth defect of the *yACT1*^S348L/WT (pseudoheterozygote) compared to *yACT1*^WT/WT at 22°C (Figure 2a,c). However, this defect was not observed when the strain was cultured at a routine temperature (30°C; Figure 2a,b). These results provide evidence that the *yACT1 S348L* variant causes a functional defect that is dominant over the wild-type allele.

6 | DISCUSSION

Baraitser–Winter cerebrofrontofacial (BWCFF; MIM#243310) syndrome, a rare monogenic disorder first described in 1988 (Baraitser & Winter, 1988), is caused by de novo missense variants in *ACTB* (MIM 102630) and *ACTG1* (MIM 102560) (Riviere et al., 2012). The cardinal features include characteristic facies (ridged metopic suture, hypertelorism, broad nasal bridge, ptosis, arched eyebrows), brain
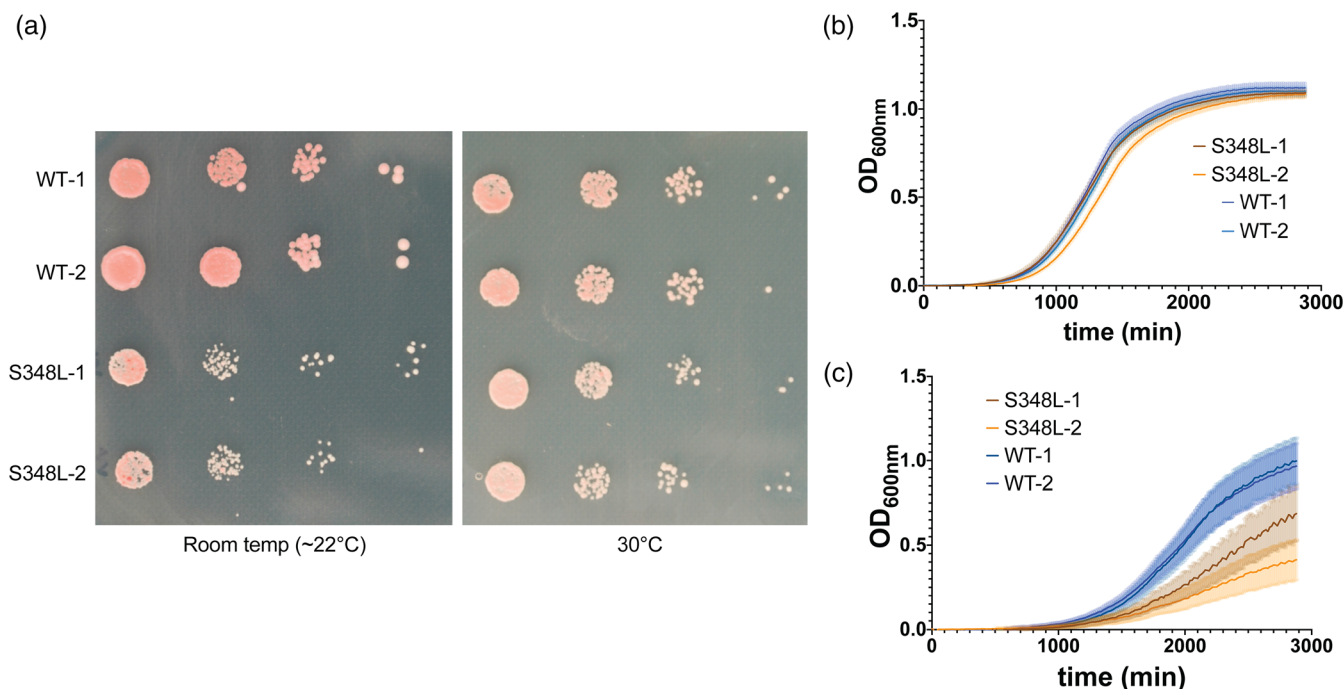

FIGURE 2 *S. cerevisiae* yACT1^S348L/WT pseudoheterozygotes exhibit growth defects at 22°C. (a) Spot tests of two independent pYCplac33: *yACT1*^WT (WT-1 and -2) and pYCplac33:*yACT1*^S348L (S348L-1 and -2) transformants grown on SD-URA plates at room temperature (~22°C) and 30°C for 4 and 2 days, respectively. Spots are (from left-to-right) progressive 10-fold serial dilutions. Growth curves of the same strains as in (a) obtained using a Bioscreen C growth analyser for incubations at (b) 30°C and (c) 22°C in SD-URA liquid medium for 48 h. The plots represent mean cell density (OD$_{600nm}$) of 10 replicates for each strain, with the shaded area illustrating 95% confidence intervals

malformations (pachygyria, lissencephaly, heterotopia), intellectual disability, ocular coloboma, and sensorineural deafness (Riviere et al., 2012; Verloes et al., 2015; Yates et al., 2017). The facial gestalt is often subtle in infancy and typically becoming more striking and assuming the commonly recognizable facies (Yates et al., 2017). The phenotypic evolution increases the diagnostic rate with age. Baraitser–Winter syndrome, Fryns–Aftimos syndrome, and cerebrofrontofacial syndromes, originally described as separate clinical entities, are now recognized through identification of the common causative genes as clinical entities within the same spectrum, explaining the phenotypic overlaps (Verloes et al., 2015; Yates et al., 2017). The phenotypic spectrum has expanded to include structural anomalies such as cleft lip and palate, and birth defects involving the heart, renal tract, gastrointestinal and musculoskeletal systems (Saskin et al., 2017; Verloes et al., 2015).

The *ACTB* gene encodes beta-actin, which is a cytoplasmic actin isoform with ubiquitous expression. It is hypothesized that the degree of gain- or loss-of-function pathogenic variants and the distribution of normal and mutant actin within cells may influence phenotypic expression (Johnston et al., 2013). The de novo variant identified in the twins reported here, with confirmed paternity and maternity, is a missense change at an amino acid residue that lies adjacent to the target binding domain within *ACTB* (Dominguez & Holmes, 2011), is absent in gnomAD, is located within an *ACTB* transcript that is intolerant to missense change, and which the majority of computational software predicting as likely to be deleterious or damaging. This indicates likelihood that Ser348Leu is a pathogenic variant, which is greatly strengthened by the functional data presented here (Richards et al., 2015). The low temperature-dependent nature of the phenotype is unusual for reported *ACT1* mutations, although a different, dominant *ACT1* mutation with a low temperature phenotype has been reported in the fission yeast, *Schizosaccharomyces pombe* (McCollum et al., 1999). While the basis for the temperature dependence remains unknown, if the human variant shows a similar temperature-dependency, it may help reveal the molecular basis for the clinical phenotype (Baliga et al., 2016).

The twins demonstrated variable expressivity with identical *ACTB* variants but different and unusual phenotypes. The main presenting feature in these identical twins was antenatal evidence of upper gastro-intestinal tract obstruction. Small intestinal atresia or stenosis is a common cause of congenital intestinal obstruction, estimated to occur in 1.6–3.4 per 10,000 live births (Lupo et al., 2017). Apple-peel bowel, or type-IIIb intestinal atresia, is a rare variant of jejunoileal atresia characterized by proximal intestinal atresia, absence of distal SMA and dorsal mesentery, and an atretic small intestine coiled around a single central artery, giving the appearance of an "apple-peel" (Louw & Barnard, 1955). The etiology of apple-peel intestinal atresia is unclear with an early vascular deficiency disrupting small bowel development and genetic causes both postulated (De Grazia et al., 2008). Monozygotic twins are known to have a much higher incidence of pregnancy complications, including vascular-related events and, indeed, the pattern of bowel abnormalities, with proximal atresia in one twin and apple-peel jejunal atresia in another, has been

reported previously in identical twins (De Grazia et al., 2008). Fetal hydrops can be secondary to small bowel atresia. However, the presence of other features in the surviving twin, notably persistent hyperglycemia beyond that expected in a preterm baby of this gestation, the phenotypic features and the presence of a critical airway indicated an underlying unifying pathology. The baby faced a protracted and complicated medical course that, in the absence of any degree of prognostic certainty, the parents were willing to embark upon. The value of ultra-rapid whole genome sequencing in providing the diagnosis that was not revealed through more traditional investigations is reinforced by this case.

Our findings raise awareness jejunal atresia with apple-peel bowel and neonatal hyperglycemia may be features of BWCFFS. We confirm for the first time that the NM_001101.3:c.1043C>T;p.(Ser348Leu) variant in *ACTB* is likely a pathogenic variant. There is one existing report of jejunal atresia with apple-peel bowel in the literature with the identical variant to that reported here; that case also exhibited hyperglycemia but no further details are available (Fakhro et al., 2019). Fetal hydrops has been described in association with different *ACTB* gene variants in two subjects who also had bowel abnormalities (Di Donato et al., 2014; Drury et al., 2015), although we cannot be confident of the cause of the hydrops in Twin 1. In addition, Twin 2 had severe laryngeal dysgenesis, which has not previously been described in association with an actin gene variant or BWCFFS. Confirmation is required that this defect is due to the variant we report.

This report demonstrates the value of rapid whole genome sequencing in the diagnosis of rare disorders in critically ill newborns. This technique also is possible in antenatal diagnosis. Rapid diagnosis provides certainty for the family in highly stressful situations in which they often are expected to contribute to major decisions about provision of care and, as in this case, may enable much better prognostication of likely outcome. Without a definitive diagnostic test, patients often embark on a series of iterative tests of escalating complexity in an attempt to find the diagnosis which may delay definitive therapeutic or palliative approaches as well as adding to cost. In this case, we report a rare case of monozygotic twins with identical de novo pathogenic missense *ACTB* variants but with variable expressivity including phenotypic features of hydrops and laryngeal dysgenesis that have not previously been reported as being associated with BWCFFS. The dysfunctional nature of the variant was confirmed through functional studies.

6.1 | Limitations

The lack of post mortem investigation of the brain in either twin, beyond MRI imaging in Twin 2, is a limitation given the prevalence of brain malformations in BWCFFS. Histological analysis of the bowel, with immunohistochemistry for beta actin, may have provided further characterization of the nature of the mutant actin but was not available. Although the functional studies provide evidence supporting categorizing the variant as a pathogenic variant, it is possible that the

variant causes developmental abnormalities in humans that are unrelated to the phenotype in single-celled yeast.

CONFLICT OF INTEREST

The authors declare that there is no conflict of interest that could be perceived as prejudicing the impartiality of the research reported.

AUTHOR CONTRIBUTIONS

Conceptualization: Kristina Sibbin, Frank Bloomfield, and Justin O'Sullivan. *Patient Clinical Assessment*: Kristina Sibbin, Frank Bloomfield, Salam Alburaiky, Raoul Heller, Stephen Evans, and Kate Strachan. *Molecular studies*: Patrick Yap, Denis Nyaga, Raoul Heller, Salam Alburaiky, Han Nguyen, Sylvie Hermann-Le Denmat, Austen Ganley, and Justin O'Sullivan. *Writing – draft preparation*: Kristina Sibbin. *Review and editing*: Kristina Sibbin, Frank Bloomfield, Patrick Yap, Denis Nyaga, Raoul Heller, Stephen Evans, Kate Strachan, Salam Alburaiky, Han Nguyen, Sylvie Hermann-Le Denmat, Austen Ganley, and Justin O'Sullivan. *Supervision*: Frank Bloomfield. All authors have read and agreed to the published version of this manuscript.

DATA AVAILABILITY STATEMENT

The data that support the molecular studies of this study are openly available in figshare at http://doi.org/10.17608.auckland.16556712, reference number https://figshare.com/s/7d3eb2592b4d5f364975. The genome sequence data for the family reported cannot be shared for privacy reasons.

ORCID

Justin M. O'Sullivan https://orcid.org/0000-0003-2927-450X
Frank H. Bloomfield https://orcid.org/0000-0001-6424-6577

REFERENCES

Baliga, C., Majhi, S., Mondal, K., Bhattacharjee, A., VijayRaghavan, K., & Varadarajan, R. (2016). Rational elicitation of cold-sensitive phenotypes. *Proceedings of the National Academy of Sciences of the United States of America*, 113, E2506–E2515. https://doi.org/10.1073/pnas.1604190113

Baraitser, M., & Winter, R. (1988). Iris coloboma, ptosis, hypertelorism, and mental retardation: A new syndrome. *Journal of Medical Genetics*, 25, 41–43. https://doi.org/10.1136/jmg.25.1.41

Dalla Vecchia, L. K., Grosfeld, J. L., West, K. W., Rescorla, F. J., & Scherer, S. A. (1998). Intestinal atresia and stenosis: A 25 year experience with 277 cases. *Archives of Surgery*, 133, 490–497. https://doi.org/10.1001/archsurg.133.5.490

De Grazia, E., Di Pace, M. R., Caruso, A. M., Catalano, P., & Cimador, M. (2008). Different types of intestinal atresia in identical twins. *Journal of Pediatric Surgery*, 43, 2301–2304. https://doi.org/10.1016/j.jpedsurg.2008.08.068

Di Donato, N., Rump, A., Koenig, R., Der Kaloustian, V. M., Halal, F., Sonntag, K., Krause, C., Hackmann, K., Hahn, G., Schrock, E., & Verloes, A. (2014). Severe forms of Baraitser–Winter syndrome are caused by ACTB mutations rather than ACTG1 mutations. *European Journal of Human Genetics*, 22, 179–183. https://doi.org/10.1038/ejhg.2013.130

Dominguez, R., & Holmes, K. C. (2011). Actin structure and function. *Annual Review of Biophysics*, 40, 169–186. https://doi.org/10.1146/annurev-biophys-042910-155359

Drury, S., Williams, H., Trump, N., Boustred, C., GOSGene, Lench, N., & Chitty, L. S. (2015). Exome sequencing for prenatal diagnosis of fetuses with sonographic abnormalities. *Prenatal Diagnosis*, 35, 1010–1017. https://doi.org/10.1002/pd.4675

Fakhro, K. A., Robay, A., Rodrigues-Flores, J. L., Mezey, J. G., Al-Shakaki, A. A., Chidiac, O., Stadler, D., Malek, J. A., Imam, A. B., Sheikh, A., Azzam, A., Janahi, I., Khanjar, I., Osman, K., Ziki, M. A., Mahmah, M. A., Selim, M., Numeiri, N., Ali, R., ... Crystal, R. G. (2019). Point of care exome sequencing reveals allelic and phenotypic heterogeneity underlying Mendelian disease in Qatar. *Human Molecular Genetics*, 28, 3970–3981. https://doi.org/10.1093/hmg/ddz134

Ganley, A. R., Ide, S., Saka, K., & Kobayashi, T. (2009). The effect of replication initiation on gene amplification in the rDNA and its relationship to aging. *Molecular Cell*, 35, 683–693. https://doi.org/10.1016/j.molcel.2009.07.012

Johnston, J. J., Wen, K. K., Keppler-Noreuil, K., McKane, M., Maiers, J. L., Greiner, A., Sapp, J. C., NIH Intramural Sequencing Center, Demali, K. A., Rubenstein, P. A., & Biesecker, L. G. (2013). Functional analysis of a de novo ACTB mutation in a patient with atypical Baraitser–Winter syndrome. *Human Mutation*, 34, 1242–1249. https://doi.org/10.1002/humu.22350

Kawai, S., Hashimoto, W., & Murata, K. (2010). Transformation of *Saccharomyces cerevisiae* and other fungi. *Bioengineered Bugs*, 1(6), 395–403. https://doi.org/10.4161/bbug.1.6.13257

Kirtane, J. M., Bhange, S. A., Nabi, F., & Shah, V. (2019). Duodenal atresia with familial apple peel syndrome: Case study with review of literature. *BMJ Case Reports*, 12, e230160. https://doi.org/10.1136/bcr-2019-230160

Louw, J. H., & Barnard, C. N. (1955). Congenital intestinal atresia: Observations on its origin. *Lancet*, 266, 1065–1067.

Lupo, P. J., Isenburg, J. L., Salemi, J. L., Mai, C. T., Liberman, R. F., Canfield, M. A., Copeland, G., Haight, S., Harpavat, S., Hoyt, A. T., Moore, C. A., Nembhard, W. N., Nguyen, H. N., Rutkowski, R. E., Steele, A., Alverson, C. J., Stallings, E. B., Kirb, R. S., & National Birth Defects Prevention Network. (2017). Population-based birth defects data in the United States, 2010–2014: A focus on gastrointestinal defects. *Birth Defects Research*, 109, 1504–1514. https://doi.org/10.1002/bdr2.1145

McCollum, D., Balasubramanian, M., & Gould, K. (1999). Identification of cold-sensitive mutations in the Schizosaccharomyces pombe actin locus. *FEBS Letters*, 451(3), 321–326. https://doi.org/10.1016/s0014-5793(99)00619-5

Richards, S., Aziz, N., Bale, S., Bick, D., Das, S., Gastier-Foster, J., Grody, W. W., Hegde, M., Lyon, E., Spector, E., Voelkerding, K., Rehm, H. L., & ACMG Laboratory Quality Assurance Committee. (2015). Standards and guidelines for the interpretation of sequence variants: A joint consensus recommendation of the American College of Medical Genetics and Genomics and the Association for Molecular Pathology. *Genetics in Medicine*, 17, 405–424. https://doi.org/10.1038/gim.2015.30

Riviere, J. B., van Bon, B. W., Hoischen, A., Kholmanskikh, S. S., O'Roak, B. J., Gilissen, C., Gijsen, S., Sullivan, C. T., Christian, S. L., Abdul-Rahman, O. A., Atkin, J. F., Chassaing, N., Drouin-Garraud, V., Fry, A. E., Fryns, J.-P., Gripp, K. W., Kempers, M., Kleefstra, T., Mancini, G. M. S., ... Dobyns, W. B. (2012). De novo mutations in the Actin genes ACTB and ACTG1 cause Baraitser–Winter syndrome.

Nature Genetics, *44*(440–444), S441–S442. https://doi.org/10.1038/ng.1091

Sadedin, S. P., Dashnow, H., James, P. A., Bahlo, M., Bauer, D. C., Lonie, A., Lunke, S., Macciocca, I., Ross, J. P., Siemering, K. R., Stark, Z., White, S. M., Melbourne Genomics Health Alliance, Taylor, G., Gaff, C., Oshlack, A., & Thorne, N. P. (2015). Cpipe: A shared variant detection pipeline designed for diagnostic settings. *Genome Medicine*, *7*, 68. https://doi.org/10.1186/s13073-015-0191-x

Sadedin, S. P., Ellis, J. A., Masters, S. L., & Oshlack, A. (2018). Ximmer: A system for improving accuracy and consistency of CNV calling from exome data. *Gigascience*, *7*, giy112. https://doi.org/10.1093/gigascience/giy112

Sandestig, A., Green, A., Jonasson, J., Vogt, H., Wahlstrom, J., Pepler, A., … Stefanova, M. (2019). Could dissimilar phenotypic effects of ACTB missense mutations reflect the actin conformational change? Two novel mutations and literature review. *Molecular Syndromology*, *9*, 259–265. https://doi.org/10.1159/000492267

Saskin, A., Tischkowitz, M., & DDD Study. (2017). Jejunal atresia, periodic fevers and psoriatic arthropathy in Baraitser–Winter malformation syndrome. *Clinical Dysmorphology*, *26*, 235–237. https://doi.org/10.1097/MCD.0000000000000197

Verloes, A., Di Donato, N., Masliah-Planchon, J., Jongmans, M., Abdul-Raman, O. A., Albrecht, B., Allanson, J., Brunner, H., Bertola, D., Chassaing, N., David, A., Devriendt, K., Eftekhari, P., Drouin-Garraud, V., Faravelli, F., Faivre, L., Giuliano, F., Almeida, L. G.,

Juncos, J., … Pilz, D. T. (2015). Baraitser–Winter cerebrofrontofacial syndrome: Delineation of the spectrum in 42 cases. *European Journal of Human Genetics*, *23*, 292–301. https://doi.org/10.1038/ejhg.2014.95

Yates, T. M., Turner, C. L., Firth, H. V., Berg, J., & Pilz, D. T. (2017). Baraitser–Winter cerebrofrontofacial syndrome. *Clinical Genetics*, *92*, 3–9. https://doi.org/10.1111/cge.12864

SUPPORTING INFORMATION

Additional supporting information may be found in the online version of the article at the publisher's website.

How to cite this article: Sibbin, K., Yap, P., Nyaga, D., Heller, R., Evans, S., Strachan, K., Alburaiky, S., Nguyen, H. (A.), Hermann-Le Denmat, S., Ganley, A. R. D., O'Sullivan, J. M., & Bloomfield, F. H. (2022). A de novo *ACTB* gene pathogenic variant in identical twins with phenotypic variation for hydrops and jejunal atresia. *American Journal of Medical Genetics Part A*, *188*A:1299–1306. https://doi.org/10.1002/ajmg.a.62631